Theoretical and Mathematical Physics, **174**(3): 421–437 (2013)

COEXISTENCE OF SUPERCONDUCTIVITY AND ANTIFERROMAGNETISM IN HEAVY-FERMION INTERMETALLIDES

© **V. V. Val'kov**[*†] **and A. O. Zlotnikov**[*]

Using the two-time retarded Green's function, we study the conditions for realizing the phase of the superconductivity and antiferromagnetism coexistence in the framework of the effective Hamiltonian for the periodic Anderson model. Such a phase was experimentally observed in rare-earth intermetallides with heavy fermions under an external pressure. In the chosen model, the Cooper instability is induced in the presence of long-range antiferromagnetic ordering as a result of the combined effect of a superexchange interaction in the subsystem of localized electrons and the hybridization between two groups of electrons. Applying an external pressure induces an increase in the energy of the localized level accompanied by an abrupt destruction of the long-range antiferromagnetic ordering in a certain region of the phase diagram. The superconductivity order parameter has a maximum value at the destruction point. We show that the decrease in the antiferromagnetic-sublattice magnetization with increasing pressure leads to a significant increase in the masses of Fermi quasiparticles, and the sign of the current carriers reverses at the critical point. The obtained results qualitatively agree well with the experimental data for the heavy-fermion intermetallide $CeRhIn_5$.

Keywords: periodic Anderson model, coexistence of superconductivity and antiferromagnetism, superexchange interaction, heavy fermion

1. Introduction

It is well known that strong electron correlations determine the properties of weakly doped copper oxides [1], [2] and heavy-fermion (HF) intermetallides [3]–[6] to a considerable degree. The nonphonon mechanism for superconducting pairing is manifested in these materials [1], [7]–[9], and Cooper instability develops either against the background of the destroyed antiferromagnetic ordering with retained short-range antiferromagnetic correlations or in the presence of the long-range antiferromagnetic ordering but with a significantly decreased sublattice magnetization.

The realization of a microscopically homogeneous phase of the coexistence of superconductivity (SC) and antiferromagnetism (AFM) in strongly correlated systems recently became a subject of increased attention. This occurred because applying an external pressure to a series of HF antiferromagnets leads to an induced phase transition with the formation of the indicated coexistence phase.

It is well known that the conditions for realizing Cooper instability in conducting antiferromagnets

[*]Kirensky Institute of Physics, Siberian Branch, RAS, Krasnoyarsk, Russia, e-mail: vvv@iph.krasn.ru, zlotn@iph.krasn.ru.

[†]Reshetnev Siberian State Aerospace University, Krasnoyarsk, Russia.

Translated from Teoreticheskaya i Matematicheskaya Fizika, Vol. 174, No. 3, pp. 484–503, March, 2013. Original article submitted June 9, 2012.

are more favorable than those in ferromagnetic metals [10], [11]. This is explained by the absence of spontaneous macroscopic magnetization and by the preservation of the degeneracy of the Fermi excitation spectrum with respect to the direction of the spin-momentum projection. Many examples of compounds in which the SC–AFM coexistence phase is observed are known. The phenomenon of simultaneous SC and AFM realization in HF systems was noted in transuranium compounds UPt_3 [12] and UPd_2Al_3 [13]. In these compounds, two of the three uranium 5f electrons are localized and are responsible for inducing antiferromagnetic ordering [14]. The third 5f electron participates in forming the HF band. The Cooper instability leading to the realization of the superconducting HF phase develops in the ensemble of such electrons.

Unlike transuranium materials, in the Ce intermetallide $CeRhIn_5$ from the group $Ce_nT_mIn_{3n+2m}$ (here, T = Co, Rh, Pd, Ir, Pt; $n = 1, 2$; $m = 0, 1$), the 4f Ce electron participates in the formation of both the long-range antiferromagnetic ordering and the Cooper instability. The entropy coincidence under the transition from the antiferromagnetic phase to the superconducting phase under external pressure indicates this indirectly [15]. In this case, the region in which SC and AFM coexist on the microscopic level is realized in the vicinity of such a transition [16]. The coexistence phase is limited by the pressure range $P \approx 1$ to 1.8 GPa with a maximum critical temperature near 2 K [15].

The strong SC–AFM interrelation was also established in copper oxides [17]. The coexistence of high-temperature SC and antiferromagnetic ordering in multilayer cuprates $HgBa_2Ca_4Cu_5O_{12+\delta}$ [18] and $Ba_2Ca_{n-1}Cu_nO_{2n}(F,O)_2$ ($n = 4, 5$) [19] was demonstrated in measurements of the Knight shift using nuclear magnetic resonance. The coexistence of the phases in the two-layer copper-oxide superconductor $YBa_2Cu_3O_{6+x}$ was shown in [20].

In connection with the foregoing, it is important to theoretically analyze the nonphonon mechanism of Cooper instability, which leads to the formation of the homogeneous superconducting phase with the *d*-wave symmetry of the order parameter on the microscopic level in the presence of long-range antiferromagnetic ordering. The problem of interpreting the anomalous behavior of the effective mass in the vicinity of the quantum phase transition can be an associated aim of such a study.

We stress that the formation of the SC–AFM coexistence phase can develop according to two scenarios. In the first scenario, two different groups of electrons are responsible for realizing the SC and AFM: the SC is established in the subsystem of itinerant fermions, while the long-range antiferromagnetic order is realized because localized electrons are present. This scenario is realized in ternary rare-earth [21] compounds and in uranium HF compounds.

The second scenario of coexistence-phase formation is manifested in cerium intermetallides. The same 4f electrons are responsible for the formation of both types of ordering in them (e.g., in $CeRhIn_5$). In this case, the effects of mutual SC and AFM influences play a more significant role and are the subject of many theoretical studies. In [22], the SC–AFM coexistence phase was studied based on the mean-field slave-boson approximation in the framework of the periodic Anderson model (PAM), which was supplemented with terms (which are quadratic in the Fermi operators) describing the Cooper instability and the instability of the antiferromagnetic state. We mention that if such an approach was used, then the question of the form of the electron–electron interaction in HF systems leading to the mixed state in which superconducting and antiferromagnetic properties are realized remained open. In [22], the region of the SC–AFM coexistence was obtained by increasing the hybridization parameter and the bandwidth of electrons. The increase in these parameters was related to an increase in an external hydrostatic pressure. In [23], SC and AFM in systems with HFs were considered more simply. The ensemble of itinerant electrons interacting with one another via the one-site Coulomb repulsion and the effective interaction leading to attraction was studied there. Additional constraints on the model were introduced to obtain the heavy effective electron mass. It was assumed that the Fermi level is in a neighborhood of the saddle point (the point X of the two-dimensional

Brillouin zone), and the presence of the logarithmic Van Hove singularity near the chemical potential was additionally assumed.

Here, based on a consistent application of the method of two-time temperature functions to the extended Anderson model, we analyze conditions in the atomic representation under which SC and AFM can coexist in strongly correlated systems with HFs. In the framework of such an approach, it is unnecessary to pass to slave bosons and to introduce an approximate description to take the constraint into account. In this case, we managed to obtain a closed self-consistent system of equations describing all required phases, including the coexistence phase, and the anomalous behavior of the effective mass of Fermi quasiparticles in the neighborhood of the quantum phase transition.

2. Hamiltonian of the electronic structure of HF intermetallides

The properties of rare-earth intermetallides with HFs are usually described using the PAM [24]–[26]. In the case of the regime of strong electron correlations, where the parameter U of the Coulomb repulsion of two electrons with the opposite spin-momentum projections localized at the same site significantly exceeds all other characteristic energies, the localized state is characterized by a single electron occupation. The atomic representation, which takes this feature explicitly into account, is the natural description in this case [27]. Here, taking processes that reflect virtual transitions of localized states to the two-electron sector of the Hilbert space into account leads to an effective Hamiltonian containing several additional terms [28], for example, terms (which are important in our further study) describing the exchange interaction in a subsystem of localized electrons. The importance of including this interaction is primarily because it can induce both the antiferromagnetic ordering and the Cooper instability. For example, it was shown in [29] that the exchange interaction in the ensemble of itinerant electrons can lead to realizing the mixed phase.

In the Wannier representation, the effective PAM Hamiltonian can be written in the form

$$\widehat{\mathscr{H}_{\text{eff}}} = \sum_{m,\sigma}(\varepsilon_0 - \mu)c^{\dagger}_{m\sigma}c_{m\sigma} + \sum_{m,l,\sigma} t_{ml}c^{\dagger}_{m\sigma}c_{l\sigma} + \sum_{m,\sigma}(E_0 - \mu)X^{\sigma\sigma}_m + \\ + \sum_{m,l,\sigma}\{(V_{ml}c^{\dagger}_{m\sigma}X^{0\sigma}_l) + (\text{H.c.})\} + \frac{1}{2}\sum_{m\neq l} J_{ml}\left(\vec{S}_m\vec{S}_l - \frac{1}{4}\widehat{N}_m\widehat{N}_l\right),$$

where $c_{m\sigma}$ and $c^{\dagger}_{m\sigma}$ are the annihilation and creation Fermi operators of an itinerant electron for the Wannier cell with the number m and the projection of the spin momentum σ; X^{rt}_m is the Hubbard operator related to the cell m, which is constructed using the atomic states $|m;r\rangle$ and $|m;t\rangle$ as usual, $X^{rt}_m = |m;r\rangle\langle t;m|$; and $\vec{S}_m$ is the quasispin vector operator of the localized subsystem, whose components are related to the operators of the atomic representation by the formulas

$$S^x_m = \frac{X^{\uparrow\downarrow}_m + X^{\downarrow\uparrow}_m}{2}, \qquad S^y_m = -i\frac{X^{\uparrow\downarrow}_m - X^{\downarrow\uparrow}_m}{2}, \qquad S^z_m = \frac{X^{\uparrow\uparrow}_m - X^{\downarrow\downarrow}_m}{2}.$$

The number operator of electrons localized at the site m is defined by $\widehat{N}_m = \sum_\sigma X^{\sigma\sigma}_m$. The model parameters are as follows: ε_0 is the one-site energy of an itinerant electron, μ is the chemical potential, t_{ml} is the matrix element of itinerant-electron hopping from the site l to the site m, E_0 is the position of the energy level of localized electrons, V_{ml} is the matrix element that describes the hybridization of the localized and itinerant states related to the same Wannier cell ($m = l$) or to different cells ($m \neq l$), and J_{ml} is the exchange interaction integral.

Assuming that the antiferromagnetic ordering can occur, we pass to the two-sublattice description. For this, as usual, we single out two types of lattice sites. In what follows, we assign sites labeled with

the subscripts $f, f', f'', \ldots$ to the first type (the sublattice F); for them, we have $\langle S_f^z \rangle > 0$ in the presence of long-range antiferromagnetic ordering. Sites of the second type (the sublattice G) are labeled with the subscripts $g, g', g'', \ldots$; we have $\langle S_g^z \rangle < 0$ for these lattice sites.

In the two-sublattice representation, it is convenient to write the Hamiltonian as

$$\widehat{\mathscr{H}_{\text{eff}}} = \widehat{\mathscr{H}_0} + \widehat{\mathscr{H}_{\text{mix}}} + \widehat{\mathscr{H}_{\text{exch}}},$$

where $\widehat{\mathscr{H}_0}$ describes the system of noninteracting localized and itinerant electrons. Using $\widehat{\mathscr{H}_{\text{mix}}}$, we take hybridization processes between the localized and itinerant electrons within one sublattice and from different sublattices into account. The term $\widehat{\mathscr{H}_{\text{exch}}}$ is responsible for the superexchange interaction in the localized subsystem. The concrete forms of these operators are

$$\begin{aligned}
\widehat{\mathscr{H}_0} = {} & \sum_{f,\sigma} (\varepsilon_0 - \mu) a_{f\sigma}^\dagger a_{f\sigma} + \sum_{g,\sigma} (\varepsilon_0 - \mu) b_{g\sigma}^\dagger b_{g\sigma} + \sum_{f,\sigma} (E_0 - \mu) X_f^{\sigma\sigma} + \\
& + \sum_{g,\sigma} (E_0 - \mu) Y_g^{\sigma\sigma} + \sum_{f,f',\sigma} t_{ff'} a_{f\sigma}^\dagger a_{f'\sigma} + \sum_{g,g',\sigma} t_{gg'} b_{g\sigma}^\dagger b_{g'\sigma} + \\
& + \sum_{f,g,\sigma} (t_{fg} a_{f\sigma}^\dagger b_{g\sigma} + t_{gf} b_{g\sigma}^\dagger a_{f\sigma}), \\
\widehat{\mathscr{H}_{\text{mix}}} = {} & \sum_{f,f',\sigma} \{(V_{ff'} a_{f\sigma}^\dagger X_{f'}^{0\sigma}) + (\text{H.c.})\} + \sum_{g,g',\sigma} \{(V_{gg'} b_{g\sigma}^\dagger Y_{g'}^{0\sigma}) + (\text{H.c.})\} + \\
& + \sum_{f,g,\sigma} \{(W_{fg} a_{f\sigma}^\dagger Y_g^{0\sigma} + W_{gf} b_{g\sigma}^\dagger X_f^{0\sigma}) + (\text{H.c.})\}, \\
\widehat{\mathscr{H}_{\text{exch}}} = {} & \frac{1}{2} \sum_{\langle fg \rangle,\sigma} J_{fg} (X_f^{\sigma\bar{\sigma}} Y_g^{\bar{\sigma}\sigma} - X_f^{\sigma\sigma} Y_g^{\bar{\sigma}\bar{\sigma}}).
\end{aligned}$$

For the operator $\widehat{\mathscr{H}_{\text{exch}}}$, we assume that the exchange interaction in the subsystem of localized states is only realized between nearest neighbors. This is reflected in the expression for $\widehat{\mathscr{H}_{\text{exch}}}$ by enclosing the site subscripts f and g on the summation sign in angle brackets. In the two-sublattice description, the parameter W_{fg} denotes the integral of hybridization of itinerant and quasilocalized states related to different sublattices. The previous notation $V_{ff'}$ and $V_{gg'}$ for the intensity of hybridization processes inside one sublattice is retained.

3. Description of the SC–AFM coexistence phase using basis operators

To obtain a closed system of self-consistent equations describing the superconducting phase, the antiferromagnetic phase, and the SC–AFM coexistence phase, we use the method of the equations of motion for two-time retarded Green's functions [30], [31]. We close the chain of equations of motion using the method of irreducible Green's functions [32], [33] and the Zwanzig–Mori projection technique [34], [35]. For this, we introduce the basis set of operators

$$\{X_f^{0\sigma}, Y_g^{0\sigma}, a_{f\sigma}, b_{g\sigma}, X_f^{\bar{\sigma}0}, Y_g^{\bar{\sigma}0}, a_{f\bar{\sigma}}^\dagger, b_{g\bar{\sigma}}^\dagger\} \tag{1}$$

and write the exact equations of motion for the first half of this set (the equations of motion for the second half are obtained from the following equations via Hermitian conjugation and the replacement $\sigma \to \bar{\sigma} = -\sigma$):

$$i\frac{dX_f^{0\sigma}}{dt} = (E_0 - \mu)X_f^{0\sigma} + \sum_{f'} V_{f'f}^*\left[(X_f^{00} + X_f^{\sigma\sigma})a_{f'\sigma} + X_f^{\bar{\sigma}\sigma}a_{f'\bar{\sigma}}\right] +$$

$$+ \sum_g W_{gf}^*[(X_f^{00} + X_f^{\sigma\sigma})b_{g\sigma} + X_f^{\bar{\sigma}\sigma}b_{g\bar{\sigma}}] + \frac{1}{2}\sum_g J_{fg}(X_f^{0\bar{\sigma}}Y_g^{\bar{\sigma}\sigma} - X_f^{0\sigma}Y_g^{\bar{\sigma}\bar{\sigma}}),$$

$$i\frac{dY_g^{0\sigma}}{dt} = (E_0 - \mu)Y_g^{0\sigma} + \sum_{g'} V_{g'g}^*[(Y_g^{00} + Y_g^{\sigma\sigma})b_{g'\sigma} + Y_g^{\bar{\sigma}\sigma}b_{g'\bar{\sigma}}] +$$

$$+ \sum_f W_{fg}^*[(Y_g^{00} + Y_g^{\sigma\sigma})a_{f\sigma} + Y_g^{\bar{\sigma}\sigma}a_{f\bar{\sigma}}] + \frac{1}{2}\sum_f J_{fg}(X_f^{\bar{\sigma}\sigma}Y_g^{0\bar{\sigma}} - X_f^{\bar{\sigma}\bar{\sigma}}Y_g^{0\sigma}),$$

$$i\frac{da_{f\sigma}}{dt} = (\varepsilon_0 - \mu)a_{f\sigma} + \sum_{f'}(t_{ff'}a_{f'\sigma} + V_{ff'}X_{f'}^{0\sigma}) + \sum_g (t_{fg}b_{g\sigma} + W_{fg}Y_g^{0\sigma}),$$

$$i\frac{db_{g\sigma}}{dt} = (\varepsilon_0 - \mu)b_{g\sigma} + \sum_{g'}(t_{gg'}b_{g'\sigma} + V_{gg'}Y_{g'}^{0\sigma}) + \sum_f (t_{gf}a_{f\sigma} + W_{gf}X_f^{0\sigma}),$$

where the asterisk denotes complex conjugation.

Projecting the right-hand sides of these equations on basis (1) and passing to the quasimomentum representation allow obtaining a closed system of eight equations for the normal and anomalous Green's functions. This system in the matrix form is written as

$$\begin{pmatrix} \widehat{M}_{p\sigma}(\omega) & \widehat{G}_{p\sigma} \\ -\widehat{G}^*_{-p\bar{\sigma}} & -\widehat{M}^*_{-p\bar{\sigma}}(-\omega) \end{pmatrix} \langle\langle \vec{A}\,|B^\dagger\rangle\rangle_\omega = \langle\{\vec{A}, B^\dagger\}_+\rangle. \tag{2}$$

The operator $\vec{A}$ contained in the vector Green's function is defined in terms of the Fourier transforms of basis operators (1):

$$\vec{A} = (X_{p\sigma}, Y_{p\sigma}, a_{p\sigma}, b_{p\sigma}, X^\dagger_{-p\bar{\sigma}}, Y^\dagger_{-p\bar{\sigma}}, a^\dagger_{-p\bar{\sigma}}, b^\dagger_{-p\bar{\sigma}}). \tag{3}$$

The operator B is chosen arbitrarily from set (3). As it usually is in the method of the two-time Green's function, if only quasi-Fermi excitations are taken into account, then the constant terms in each equation are determined by the thermodynamic average $\langle\,\cdot\,\rangle$ of the anticommutator $\{\,\cdot\,,\,\cdot\,\}_+$ of the component of the vector $\vec{A}$ and the operator B. In Eqs. (2), we assume that $\langle AB^\dagger\rangle^* = \langle BA^\dagger\rangle$.

In what follows, the averages of the anticommutators of the Hubbard operators in the quasimomentum representation play a significant role:

$$\langle\{X_{p\sigma}, X^\dagger_{p\sigma}\}_+\rangle = \langle\{Y_{p\bar{\sigma}}, Y^\dagger_{p\bar{\sigma}}\}_+\rangle = \alpha_\sigma, \qquad \alpha_\sigma = 1 - \frac{n_{\mathrm{L}}}{2} + \eta_\sigma R,$$

where $R = \langle S_f^z\rangle$ is the magnetization of the sublattice F and $\langle N_f\rangle = \langle N_g\rangle = n_{\mathrm{L}}$ is the average number of electrons at the localized level. The σ-dependent function η_σ is defined as usual: $\eta_\sigma = \pm 1$ if respectively

$\sigma = \pm 1/2$. The fourth-order matrices introduced in (2) are given by

$$\widehat{M}_{p\sigma}(\omega) = \begin{pmatrix} \omega - E_\sigma & L_p/\alpha_{\bar\sigma} & -\alpha_\sigma V_p^* & -\alpha_\sigma W_p^* \\ L_p/\alpha_\sigma & \omega - E_{\bar\sigma} & -\alpha_{\bar\sigma} W_p^* & -\alpha_{\bar\sigma} V_p^* \\ -V_p & -W_p & \omega - \xi_p & -\Gamma_p \\ -W_p & -V_p & -\Gamma_p & \omega - \xi_p \end{pmatrix},$$

$$\widehat{G}_{p\sigma} = -\begin{pmatrix} \eta_\sigma \Phi/\alpha_{\bar\sigma} & \eta_\sigma \Delta_p/\alpha_\sigma & 0 & 0 \\ \eta_\sigma \Delta_{-p}/\alpha_{\bar\sigma} & \eta_\sigma \Phi/\alpha_\sigma & 0 & 0 \\ 0 & 0 & 0 & 0 \\ 0 & 0 & 0 & 0 \end{pmatrix}.$$

In these formulas, the renormalized expression for the energy of the localized level,

$$E_\sigma = E_0 - \mu - J(n_{\mathrm{L}} + 2\eta_\sigma R) - \Lambda_\sigma + C_\sigma, \tag{4}$$

describes the mean-field effect of the exchange interaction leading to both the level displacement (the contribution proportional to $-Jn_{\mathrm{L}}$) and the removal of the degeneracy of this level with respect to the spin-momentum projection (the contribution proportional to $-2\eta_\sigma JR$). The third term,

$$\Lambda_\sigma = \frac{1}{\alpha_\sigma} \cdot \frac{1}{N} \sum_k \{V_k^* \langle X_{k\bar\sigma}^\dagger a_{k\bar\sigma} \rangle + W_k^* \langle X_{k\bar\sigma}^\dagger b_{k\bar\sigma} \rangle\},$$

appears because of the combined effects of the kinematic and hybridization interactions. The kinematic interaction is a consequence of the non-Fermi character of the permutation relations for the Hubbard operators [36], [37] describing the subsystem of f electrons. The last term in renormalized expression (4) for the energy,

$$C_\sigma = \frac{1}{\alpha_\sigma} \cdot \frac{1}{2N} \sum_k J_k C_{k\sigma}, \tag{5}$$

is related to the inclusion of static magnetic fluctuations and fluctuations of the value of the f level occupation. These fluctuations via the exchange coupling mechanism lead to the displacement of the localized level dependent on the spin-momentum projection. The quantity $C_{k\sigma}$ in (5) is the Fourier transform of the spatial correlator

$$C_{fg}^\sigma = \langle X_f^{\sigma\bar\sigma} Y_g^{\bar\sigma\sigma} \rangle + \frac{1}{4} \langle \widehat{N}_f \widehat{N}_g \rangle + \langle S_f^z S_g^z \rangle - \left(\frac{1}{4} n_{\mathrm{L}}^2 - R^2 \right) \tag{6}$$

and is given by the equality

$$C_{fg}^\sigma = \frac{1}{N} \sum_k e^{ik(f-g)} C_{k\sigma}.$$

In formula (6), we take into account that $\langle X_f^{\uparrow\uparrow} Y_g^{\uparrow\uparrow} \rangle = \langle X_f^{\downarrow\downarrow} Y_g^{\downarrow\downarrow} \rangle$.

The joint effect of the kinematic and exchange interactions in the subsystem of localized fermions leads to the appearance of the effective coupling between the localized states from different sublattices (there were no corresponding terms in the initial Hamiltonian). The intensity of such a mixing is determined by the function L_p, which is expressed in terms of the kinetic correlators:

$$L_p = \frac{1}{2N} \sum_k J_{p-k} \langle Y_{k\uparrow}^\dagger X_{k\uparrow} \rangle.$$

As is known, the appearance of the superconducting state is described mathematically by introducing anomalous averages of the Fermi and quasi-Fermi operators. The presence of the hybridization, exchange, and kinematic interactions in the extended Anderson model leads to the possibility of realizing two types of anomalous averages. Accordingly, two superconducting order parameters (SOPs) appear in the theory. The first SOP,

$$\Phi = \frac{1}{N}\sum_{k,\sigma}\eta_\sigma(V_k^*\langle a_{k\sigma}X_{-k\bar{\sigma}}\rangle + W_k^*\langle b_{k\sigma}X_{-k\bar{\sigma}}\rangle),$$

is related to the anomalous pairings of the itinerant and localized electrons, which are induced by the joint effect of the hybridization and kinematic interactions. The second SOP is a result of the Cooper pairing of quasilocalized fermions from different sublattices and is due to the dynamical part of the exchange interaction:

$$\Delta_p = \frac{1}{2N}\sum_k J_{p-k}(\langle X_{k\uparrow}Y_{-k\downarrow}\rangle + \langle Y_{-k\uparrow}X_{k\downarrow}\rangle). \tag{7}$$

The quantity $\xi_p = \varepsilon_0 + t_p - \mu$ corresponds to the part of the kinetic energy of the itinerant electrons (measured from the chemical potential μ) that is related to intrasublattice hopping. The functions t_p, Γ_p, V_p, and W_p are defined in terms of the Fourier transforms of the intrasublattice and intersublattice hopping and hybridization parameters:

$$t_{ff'} = \frac{1}{N}\sum_k e^{ik(f-f')}t_k, \qquad t_{fg} = \frac{1}{N}\sum_k e^{ik(f-g)}\Gamma_k,$$

$$V_{ff'} = \frac{1}{N}\sum_k e^{ik(f-f')}V_k, \qquad W_{fg} = \frac{1}{N}\sum_k e^{ik(f-g)}W_k.$$

When projecting the equations of motion on basis operator set (1), we take the obvious relation between the anomalous averages $\langle X_f^{0\sigma}a_{f'\bar{\sigma}}\rangle$ and $\langle X_f^{0\sigma}b_{g\bar{\sigma}}\rangle$ and the anomalous averages $\langle Y_g^{0\sigma}b_{g'\bar{\sigma}}\rangle$ and $\langle Y_g^{0\sigma}a_{f\bar{\sigma}}\rangle$ into account. The corresponding formulas are obtained based on simple symmetry considerations. Applying the translation operation translating the sites of the sublattice F to those of the sublattice G and the inversion of the quantization axis z, we find that $\langle Y_g^{0\sigma}b_{g'\bar{\sigma}}\rangle = -\langle X_f^{0\bar{\sigma}}a_{f'\sigma}\rangle$ and $\langle Y_g^{0\sigma}a_{f\bar{\sigma}}\rangle = -\langle X_f^{0\bar{\sigma}}b_{g\sigma}\rangle$. In this case, the transformation law for the spinor quantities under the rotation about the axis x,

$$c_{l\sigma} \to c_{l\sigma}(\theta) = e^{i\theta s_l^x}c_{l\sigma}e^{-i\theta s_l^x} = c_{l\sigma}\cos\frac{\theta}{2} - ic_{l\bar{\sigma}}\sin\frac{\theta}{2},$$

$$X_l^{0\sigma} \to X_l^{0\sigma}(\theta) = e^{i\theta S_l^x}X_l^{0\sigma}e^{-i\theta S_l^x} = X_l^{0\sigma}\cos\frac{\theta}{2} - iX_l^{0\bar{\sigma}}\sin\frac{\theta}{2},$$

is used.

4. Irreducible Green's functions and self-consistent equations

The type of SOP symmetry is important in the study of the SC–AFM coexistence. This question is currently open for systems with HFs. The Fourier transforms of the exchange integrals $J_{p\pm k}$ in definition (7) can lead to a dependence of the SOP Δ_p on the quasimomentum corresponding to various types of SOP symmetry. For the magnetic Brillouin zone transformed by rotating through the angle $\pi/4$ about the initial Brillouin zone, the dependence of the SOP corresponding to the s-type symmetry becomes $\Delta_p^s = 2\Delta_0^s\cos(p_xb/2)\cos(p_yb/2)$. The decrease in the Brillouin zone is related to the transition to a new unit cell with the parameter $b = \sqrt{2}a$ of the lattice with two antiferromagnetic sublattices. In the transformed coordinate system, the dependence of the SOP for the d-type symmetry is $\Delta_p^d = 2\Delta_0^d\sin(p_xb/2)\sin(p_yb/2)$.

We note that for the compound $CeRhIn_5$, the d-type SOP symmetry is assumed more preferable [38]. Therefore, in what follows, we restrict ourself to studying the SC–AFM joint effect with this type of order parameter symmetry.

Choosing this type of SOP symmetry leads to simplification of the self-consistent equations because the anomalous order parameter Φ only contributes to the s-type symmetry. Therefore, we assume that $\Phi = 0$ below.

When writing solutions of Eqs. (2) for the Green's function in the SC–AFM coexistence phase, we use the notation

$$d_{3\sigma}(p,\omega) = (\omega + E_\sigma)\big((\omega+\xi_p)^2 - \Gamma_p^2\big) - \alpha_\sigma(\omega+\xi_p)(V_p^2 + W_p^2) + 2\alpha_\sigma\Gamma_p V_p W_p, \tag{8}$$

$$f_3(p,\omega) = \frac{L_p}{\alpha_\sigma\alpha_{\bar\sigma}}\big((\omega+\xi_p)^2 - \Gamma_p^2\big) + 2(\omega+\xi_p)V_pW_p - \Gamma_p(V_p^2+W_p^2), \tag{9}$$

$$d_4(p,\omega) = (\omega+E_{\bar\sigma})d_{3\sigma}(p,\omega) + (\omega+E_\sigma)\,d_{3\bar\sigma}(p,\omega) + \alpha_\sigma\alpha_{\bar\sigma}(V_p^2 - W_p^2)^2 -$$

$$- \left((\omega+E_\sigma)(\omega+E_{\bar\sigma}) - \frac{L_p^2}{\alpha_\sigma\alpha_{\bar\sigma}}\right)\big((\omega+\xi_p)^2 - \Gamma_p^2\big) - 2L_pf_3(p,\omega). \tag{10}$$

The equation $d_4(p,-\omega) = 0$ determines the system energy spectrum in the case of the normal antiferromagnetic phase where the anomalous averages are not taken into account.

The expressions for normal Green's functions are written as

$$\langle\langle X_{p\sigma}|X_{p\sigma}^\dagger\rangle\rangle_\omega = -\frac{\alpha_\sigma S_{p\sigma}(\omega)}{D_8(p,\omega)}, \qquad \langle\langle a_{p\sigma}|a_{p\sigma}^\dagger\rangle\rangle_\omega = \frac{C_{p\sigma}(\omega)}{D_8(p,\omega)}, \tag{11}$$

where

$$S_{p\sigma}(\omega) = d_{3\bar\sigma}(p,-\omega)d_4(p,\omega) + \left(\frac{\Delta_p}{\alpha_{\bar\sigma}}\right)^2\big((\omega-\xi_p)^2 - \Gamma_p^2\big)d_{3\sigma}(p,\omega),$$

$$C_{p\sigma}(\omega) = \left((\omega-E_\sigma)(\omega-E_{\bar\sigma}) - \frac{L_p^2}{\alpha_\sigma\alpha_{\bar\sigma}}\right)(\omega-\xi_p)d_4(p,\omega) -$$

$$- \big(\alpha_{\bar\sigma}V_p^2(\omega-E_\sigma) + \alpha_\sigma W_p^2(\omega-E_{\bar\sigma}) - 2L_pV_pW_p\big)\,d_4(p,\omega) -$$

$$- \left(\frac{\Delta_p}{\alpha_{\bar\sigma}}\right)^2\big((\omega-E_\sigma)(\omega-\xi_p) - \alpha_\sigma W_p^2\big)\,d_{3\sigma}(p,\omega) -$$

$$- \left(\frac{\Delta_p}{\alpha_\sigma}\right)^2\big((\omega-E_{\bar\sigma})(\omega-\xi_p) - \alpha_{\bar\sigma}V_p^2\big)\,d_{3\bar\sigma}(p,\omega) -$$

$$- 2\Delta_p^2\left(V_pW_p - \frac{L_p}{\alpha_\sigma\alpha_{\bar\sigma}}(\omega-\xi_p)\right)f_3(p,\omega) + \frac{\Delta_p^4(\omega-\xi_p)}{(\alpha_\sigma\alpha_{\bar\sigma})^2}\big((\omega+\xi_p)^2 - \Gamma_p^2\big).$$

In view of the equivalence between the antiferromagnetic sublattices, we have the equalities of the Green's functions $\langle\langle X_{p\sigma}|X_{p\sigma}^\dagger\rangle\rangle_\omega = \langle\langle Y_{p\bar\sigma}|Y_{p\bar\sigma}^\dagger\rangle\rangle_\omega$ and $\langle\langle a_{p\sigma}|a_{p\sigma}^\dagger\rangle\rangle_\omega = \langle\langle b_{p\bar\sigma}|b_{p\bar\sigma}^\dagger\rangle\rangle_\omega$.

When writing the anomalous Green's functions, we introduce the additional notation

$$Q_{p\sigma}(\omega) = \frac{1}{\alpha_{\bar\sigma}}\,d_{3\sigma}(p,\omega)d_{3\sigma}(p,-\omega) + \alpha_{\bar\sigma}f_3(p,\omega)f_3(p,-\omega),$$

$$R_{p\sigma}(\omega) = \frac{1}{\alpha_\sigma^2\alpha_{\bar\sigma}}\big((\omega+\xi_p)^2 - \Gamma_p^2\big)\big((\omega-\xi_p)^2 - \Gamma_p^2\big).$$

The anomalous Green's function is then written as

$$\langle\langle Y_{-p\bar{\sigma}} \,|\, X_{p\sigma} \rangle\rangle_{\omega} = -\eta_{\bar{\sigma}}\alpha_{\sigma}\frac{\Delta_p Q_{p\bar{\sigma}}(\omega) + \Delta_p^3 R_{p\bar{\sigma}}(\omega)}{D_8(p,\omega)}. \tag{12}$$

We note that the numerator of expression (12) contains only even powers of ω.

The dispersion equation in the SC–AFM coexistence phase is determined by the condition for the presence of poles of the Green's function and has the form

$$\begin{aligned} 0 = D_8(p,\omega) = d_4(p,\omega)d_4(p,-\omega) + \left(\frac{\Delta_p}{\alpha_{\bar{\sigma}}}\right)^2 d_{3\sigma}(p,\omega)d_{3\sigma}(p,-\omega) + \\ + \left(\frac{\Delta_p}{\alpha_{\sigma}}\right)^2 d_{3\bar{\sigma}}(p,\omega)d_{3\bar{\sigma}}(p,-\omega) + 2\Delta_p^2 f_3(p,\omega)f_3(p,-\omega) + \\ + \left(\frac{\Delta_p^2}{\alpha_{\sigma}\alpha_{\bar{\sigma}}}\right)^2 \big((\omega-\xi_p)^2 - \Gamma_p^2\big)\big((\omega+\xi_p)^2 - \Gamma_p^2\big). \end{aligned} \tag{13}$$

The averages $\langle X_f^{\sigma\sigma}\rangle$ in the definitions of the concentration n_{L} of localized quasiparticles and the magnetization R can be related to Green's functions (11) using the spectral theorem (for different projection directions of the spin momentum σ). Therefore, such averages are determined by the self-consistent equations

$$\langle X_f^{\sigma\sigma}\rangle = \frac{1}{N}\sum_{k,j}\alpha_{\sigma}\frac{S_{k\sigma}(-E_{jk})f(-E_{jk}/T) - S_{k\sigma}(E_{jk})f(E_{jk}/T)}{2E_{jk}\prod_{i\neq j}(E_{jk}^2 - E_{ik}^2)},$$

where $f(x) = 1/(e^x+1)$ is the Fermi–Dirac distribution function and the subscripts j and i range from 1 to 4, which corresponds to four positive-definite branches of the energy spectrum E_{jk} found from dispersion equation (13). Hence, the quantities n_{L} and R are defined as

$$n_{\mathrm{L}} = \langle X_f^{\uparrow\uparrow}\rangle + \langle X_f^{\downarrow\downarrow}\rangle, \qquad R = \frac{\langle X_f^{\uparrow\uparrow}\rangle - \langle X_f^{\downarrow\downarrow}\rangle}{2}.$$

The concentration of itinerant quasiparticles is given by the formula

$$n_{\mathrm{c}} = \frac{1}{N}\sum_{k,\sigma}\langle a_{k\sigma}^{\dagger}a_{k\sigma}\rangle, \tag{14}$$

where the average is expressed via the definition of the Green's function in (11):

$$\langle a_{p\sigma}^{\dagger}a_{p\sigma}\rangle = \sum_{j}\frac{C_{p\sigma}(E_{jp})f(E_{jp}/T) - C_{p\sigma}(-E_{jp})f(-E_{jp}/T)}{2E_{jp}\prod_{i\neq j}(E_{jp}^2 - E_{ip}^2)}.$$

Writing the expression for the total number of electrons in the system

$$N_{\mathrm{e}} = \sum_{f,\sigma}\big(\langle X_f^{\sigma\sigma}\rangle + \langle a_{f\sigma}^{\dagger}a_{f\sigma}\rangle\big) + \sum_{g,\sigma}\big(\langle Y_g^{\sigma\sigma}\rangle + \langle b_{g\sigma}^{\dagger}b_{g\sigma}\rangle\big),$$

we find that the self-consistent equation for the chemical potential can be expressed in terms of the site concentration of localized and itinerant electrons: $n_{\mathrm{e}} = N_{\mathrm{e}}/2N = n_{\mathrm{L}} + n_{\mathrm{c}}$.

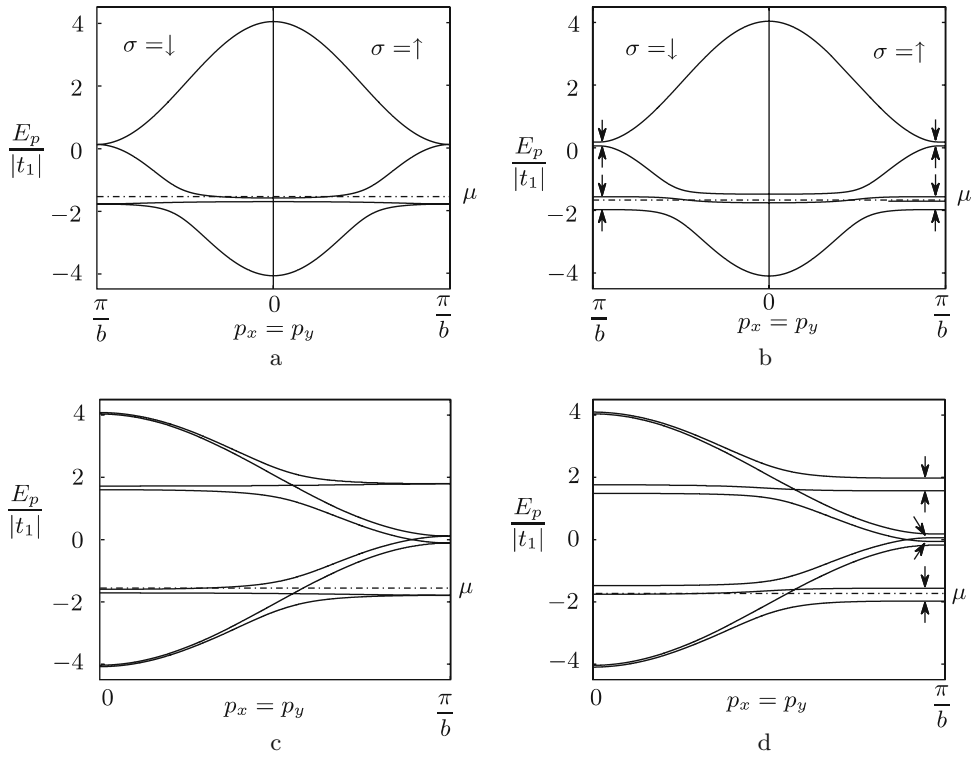

Fig. 1. Quasiparticle spectrum in the PAM found (a), (b) from the equation $d_4(p, -\omega) = 0$ (see (10)) and (c), (d) from Eq. (13) for $J = 0.2$, $V_0 = 0.6$, and $E_0 = -1.5$: the graphs show the spectra (a), (c) for the normal paramagnetic phase ($\Delta_0^d = 0$ and $R = 0$) in the case where $n_e = 1.4$, $\mu = -1.554$, and $n_L = 0.907$ and (b), (d) for the normal antiferromagnetic phase ($\Delta_0^d = 0$ and $R = 0.364$) in the case where $n_e = 1.2$, $\mu = -1.706$, and $n_L = 0.746$.

We substitute $\Delta_p = 2\Delta_0^d \sin(p_x b/2)\sin(p_y b/2)$ in the integral self-consistent equation obtained from definition (7). Using the spectral theorem for anomalous Green's function (12), we obtain an algebraic equation for the amplitude Δ_0^d of anomalous pairing:

$$1 = 2J\frac{1}{N}\sum_k \left[\sin\left(\frac{k_x b}{2}\right)\sin\left(\frac{k_y b}{2}\right)\right]^2 \sum_j \frac{-Q_k(E_{jk})\tanh(E_{jk}/2T)}{2E_{jk}\prod_{i\neq j}(E_{jk}^2 - E_{ik}^2)} +$$

$$+ 8J(\Delta_0^d)^2\frac{1}{N}\sum_k \left[\sin\left(\frac{k_x b}{2}\right)\sin\left(\frac{k_y b}{2}\right)\right]^4 \sum_j \frac{-R_k(E_{jk})\tanh(E_{jk}/2T)}{2E_{jk}\prod_{i\neq j}(E_{jk}^2 - E_{ik}^2)},$$

where

$$Q_p(\omega) = \sum_\sigma \alpha_\sigma Q_{p\bar{\sigma}}(\omega), \qquad R_p(\omega) = \sum_\sigma \alpha_\sigma R_{p\bar{\sigma}}(\omega).$$

5. Quasiparticle bands in the SC–AFM coexistence phase

The determinant $d_4(p, \omega)$ is independent of the direction of the projection of the electron spin momentum σ. This is evidence that the spectra of Fermi excitations in the antiferromagnetic phase for quasiparticles with the spin-momentum directions $\sigma = \uparrow$ and $\sigma = \downarrow$ are equivalent. It is easy to see that the determinant $D_8(p, \omega)$ is also independent of the direction of the spin-momentum projection.

If we set $\Delta_p = 0$ in complete dispersion equation (13), then the dispersion equation corresponds to the case of the normal phase (the equation $d_4(p, -\omega) = 0$). In the superconducting phase, the dispersion equation has four additional solutions. Their appearance is shown in Fig. 1 with the spectrum of quasiparticle bands in the PAM along the main direction of the Brillouin zone for the concentrations $n_e = 1.4$ (Figs. 1a and 1c) and $n_e = 1.2$ (Figs. 1b and 1d). The model energy parameters $J = 0.2$, $V_0 = 0.6$, and $E_0 = -1.5$ are normalized to $|t_1|$. The parameters Λ_σ, C_σ, and L_p are assumed to be zero. We choose such model parameters, for which the system is in the normal phase, to simplify the comparison.

The solutions of the equation $d_4(p, -\omega) = 0$ for $n_e = 1.4$ in the case of different projection directions of the quasiparticle spin momentum are shown in Fig. 1a. For such a concentration, the self-consistent calculation only leads to the trivial solution for the magnetization $R = 0$ and to the values $n_L = 0.907$ and $\mu = -1.554$. The dot-dashed line in Fig. 1 shows the level of the chemical potential μ. The change in the concentration can induce the transition to the antiferromagnetic phase. For example, the long-range antiferromagnetic order with the parameters $R = 0.364$, $n_L = 0.746$, and $\mu = -1.706$ is realized in the system for the concentration $n_e = 1.2$ (see Fig. 1b). The lower two arrows in the right and left parts of Fig. 1b indicate that the quasiparticle bands move apart; this is caused by the exchange field of spin momenta of localized electrons. The separation of branches corresponding to the states of band electrons (the upper pair of arrows) is due to hybridization processes with antiferromagnetically ordered localized electrons. The form of quasiparticle bands shown in Fig. 1a and Fig. 1b is typical of the two-sublattice PAM (see, e.g., [39]).

The solutions of Eq. (13) for the same parameters as in Figs. 1a and 1b are respectively shown in Figs. 1c and 1d. The appearance of additional branches is related to the fact that the anomalous Green's functions are constructed with operators with different directions of the quasiparticle spin momentum. In this case, the total energy spectrum in the SC–AFM coexistence problem contains four energy branches of the HF antiferromagnet for quasiparticles with $\sigma = \uparrow$ and four branches in the case $\sigma = \downarrow$ taken with the opposite sign.

In the general case, the analytic form of solutions of dispersion equation (13) is rather awkward and is not presented here. In practice, it is important to have at least approximate, but analytic, expressions for the quasiparticle spectrum in a neighborhood of the energy E_0 of localized states. The dispersion dependence of the HF band is determined in terms of precisely them.

The determination of the approximate solution is related to the replacement $\omega - \xi_p \to E_J - \mu - \xi_p$ in Eq. (13). Here, we use the notation $E_J = E_0 - Jn_L$. The described approximation is applicable for a small splitting of the HF band in the antiferromagnetic phase when $4JR \ll W$ [40], where W is the bandwidth of itinerant electrons. For simplicity, we restrict ourself to considering only intrasublattice hybridization ($W_p = 0$) and also to the nearest-neighbor approximation with respect to the electron hopping. In what follows, the energy is measured from the level ε_0, i.e., it is assumed that $\varepsilon_0 = 0$. In this case,

$$[E_p^{\mathrm{HF}}]^2 = \big((1-\alpha\gamma_p)E_J\big)^2 + (\alpha^2 - R^2)\Gamma_p^2\gamma_p^2 + (\gamma_p E_J + 2J)^2R^2 + \\ + \frac{\alpha^2 + R^2}{(\alpha^2 - R^2)^2}\Delta_p^2 + 2\,\mathrm{sgn}(\gamma_p)\nu_p^2, \qquad \gamma_p = \frac{V_p^2}{\Gamma_p^2 - E_J^2}. \tag{15}$$

The superscript HF indicates that (15) only describes the spectrum of the HF band. The function $\mathrm{sgn}(\,\cdot\,)$ is determined standardly: $\mathrm{sgn}(\gamma_p) = \pm 1$ if $\gamma_p \gtrless 0$. We also introduce the notation

$$\nu_p^4 = \left((\alpha^2 - R^2)\big((1-\alpha\gamma_p)E_J\big)^2 + \frac{\Delta_p^2 R^2}{\alpha^2 - R^2}\right)\Gamma_p^2\gamma_p^2 + \\ + \left(\big((1-\alpha\gamma_p)E_J\big)(\gamma_p E_J + 2J) + \frac{\alpha\Delta_p^2}{(\alpha^2 - R^2)^2}\right)^2 R^2.$$

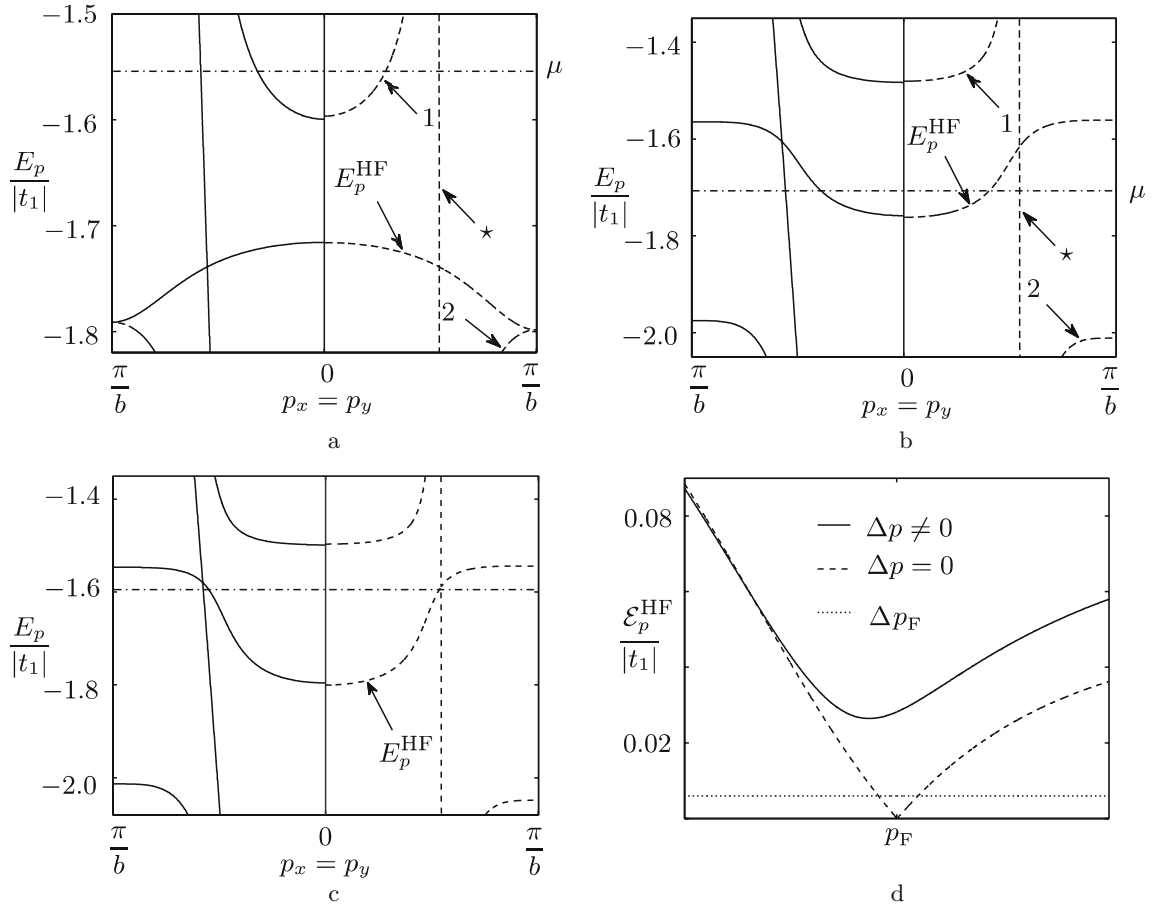

Fig. 2. Spectrum of the HF band $E_p^{\rm HF}$ in the PAM: (a) the normal paramagnetic phase $n_{\rm e} = 1.4$ and (b) the normal antiferromagnetic phase $n_{\rm e} = 1.2$. The parameters in the upper graphs are the same as in the respective Figs. 1a and 1b. (c) The SC–AFM coexistence phase $n_{\rm e} = 1.35$, $R = 0.411$, $\Delta_0^d = 0.00514$, $n_{\rm L} = 0.871$, and $\mu = -1.595$ and (d) the spectrum of elementary excitations in the coexistence phase.

The region including the HF band in Figs. 1a and 1b is given in Figs. 2a and 2b on an expanded scale. Exact solutions of Eq. (13) are shown by solid lines in the left half of each of the graphs in Fig. 2. In the right half, the dashed line marked by $E_p^{\rm HF}$ corresponds to the solution calculated using formula (15). The analytic expression for the spectrum of quasiparticle bands denoted by 1 and 2 can be obtained from (15) if the sign of the term $2\,{\rm sgn}(\gamma_p)\nu_p^2$ is reversed. It can be seen that the approximate analytic solution agrees well with the exact one calculated numerically. The dashed line marked by the $\star$ does not correspond to a real band and is shown for clarity.

The spectrum of quasiparticle bands for the concentration $n_{\rm e} = 1.35$ corresponding to the SC–AFM coexistence phase is shown in Fig. 2c. The parameters of such a phase are $R = 0.411$, $\Delta_0^d = 0.00514$, $n_{\rm L} = 0.871$, and $\mu = -1.595$. The formation of the superconducting gap in the spectrum of elementary excitations for such parameters is shown in Fig. 2d. Here, the energy $\mathcal{E}_p^{\rm HF}$ is measured from the Fermi energy, and $p_{\rm F}$ is the Fermi momentum for the zero SOP. The value $\Delta_{p_{\rm F}}$, shown by the dotted line in the graph, determines the amplitude of anomalous pairings at the Fermi surface. It can be seen that the actual size of the superconducting gap in the spectrum significantly exceeds $\Delta_{p_{\rm F}}$ because the HF spectrum has a more complicated form than the energy spectrum in the Bardeen–Cooper–Schrieffer theory. Therefore, the

SOP not only is determined by the amplitude Δ_p of superconducting pairings but also depends on other model parameters. To find the SOP that corresponds to the size of the superconducting gap more precisely than $\Delta_{p_{\rm F}}$, we give the approximate expression for the HF energy spectrum:

$$\mathcal{E}_p^{\rm HF} \approx \sqrt{(\mathcal{E}_p^{\rm AFM})^2 + \zeta_p \Delta_p^2},$$

where

$$\zeta_p = \frac{\alpha^2 + R^2}{(\alpha^2 - R^2)^2} - \frac{R^2}{(\alpha^2 - R^2)|(1-\alpha\gamma_p)E_J - \mu|\lambda_p} \times$$
$$\times \left(\Gamma_p^2 \gamma_p^2 + \frac{2\alpha}{\alpha^2 - R^2}\big((1-\alpha\gamma_p)E_J - \mu\big)(\gamma_p E_J + 2J)\right),$$
$$\mathcal{E}_p^{\rm AFM} = |(1-\alpha\gamma_p)E_J - \mu| - \lambda_p, \qquad \lambda_p = \sqrt{(\alpha^2 - R^2)\Gamma_p^2\gamma_p^2 + (\gamma_p E_J + 2J)^2 R^2}.$$

It is easy to show that the true SOP has the form $\Psi_p = \sqrt{\zeta_p}\Delta_p$. But the transition from the superconducting to the normal phase is determined by the condition $\Delta_p = 0$ as before. In this case, the quantity Δ_p can be determined as the SOP, but it does not correspond to the actual size of the gap in the spectrum.

As mentioned above, approximate expression (15) corresponds to the spectrum of the band of HFs whose effective mass exceeds that of Bloch electrons in the lattice. It is essential that realizing the long-range antiferromagnetic order and SC requires the chemical potential to be in the weak-dispersion band of the HFs. Therefore, the antiferromagnetic and superconducting characteristics of the system are determined by precisely HFs. To estimate the effective mass of new quasiparticles, we expand spectrum (15) in a neighborhood of the point $(p_x, p_y) = (0, 0)$. The mass of HFs whose energy bands $E_p^{\rm HF}$ are shown in Figs. 2a– 2c near the band bottom is given by

$$\frac{m_{\rm HF}}{m_0} = \frac{\Gamma_0^2 - E_J^2}{|\Gamma_0|\gamma_0}\left(2\alpha|E_J| - \frac{(\alpha^2 - R^2)\Gamma_0^2\gamma_0 + (\alpha^2 + R^2)E_J^2\gamma_0 - J_0 R^2|E_J|}{\lambda_0}\right)^{-1}, \tag{16}$$

where $m_0 = \hbar^2/|t_1|b^2$ is the mass of the Bloch electron in the square lattice. The quantities Γ_0 and γ_0 are obtained from the known Γ_p and γ_p for $p_x = 0$ and $p_y = 0$. Such a procedure (but in the framework of the slave-boson representation) was used in [40] to estimate the HF mass for antiferromagnetic intermetallides in the case where the canting of the antiferromagnetic sublattices was taken into account.

6. Coexistence of SC and AFM in HF systems

The change in the type of ground PAM state (at zero temperature) as a function of the total concentration $n_{\rm e}$ of carriers in the system is shown in Fig. 3 for the fixed parameters $J = 0.2$, $V_0 = 0.6$, and $E_0 = -1.5$. The solid line shows the sublattice magnetization R (left scale), and the dot-dashed line shows the amplitude Δ_0^d of the anomalous pairings corresponding to the d-type symmetry (right scale). The results of calculating Δ_0^d at zero magnetization are given for comparison and are shown by the dotted line. The states whose energy structure is shown in Figs. 2a, 2b, and 2c are marked by the respective numbers 1, 2, and 3 in the graph. It can be seen that the position of the chemical potential with respect to the HF band is important for the concentration dependence of the magnetization and the SOP amplitude.

The process can be described qualitatively as follows. As the number of electrons increases because the localized level becomes occupied, the long-range antiferromagnetic order is induced in the system. But a subsequent increase in the concentration leads to a sharp AFM suppression. This is related to the fact that the level becomes almost filled, and new added electrons form an itinerant subsystem. The enhancement

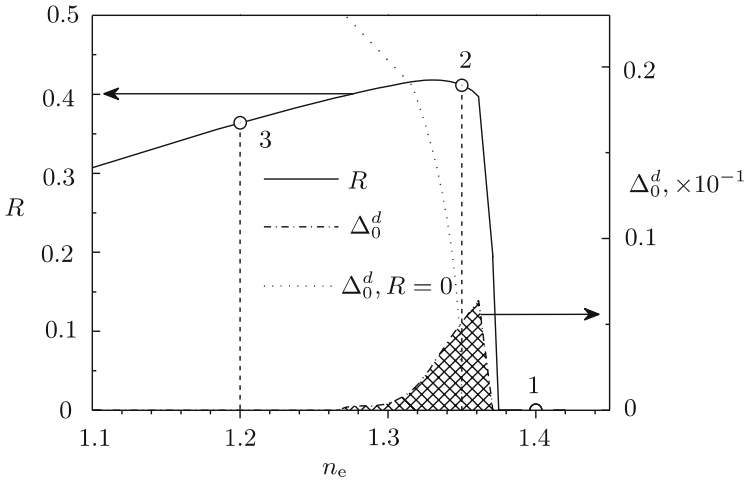

Fig. 3. Dependence of the sublattice magnetization R and the SOP amplitude Δ_0^d on the total concentration n_e of carriers in the system: the model parameters are $J = 0.2$, $V_0 = 0.6$, and $E_0 = -1.5$.

of hybridization processes in such a case is responsible for the AFM destruction. As shown in Fig. 3, near the transition from the antiferromagnetic to the paramagnetic phase, Cooper instability is realized in the system. This leads to the appearance of the SC–AFM coexistence phase. The shaded region in Fig. 3 determines the concentrations in the case where Cooper instability and long-range antiferromagnetic order coexist.

We note that the phases are limited not by temperatures but by concentrations in our consideration. The presence of the long-range antiferromagnetic order in the subsystem of localized Hubbard fermions can induce superconducting pairings. This follows because the increase or decrease in the magnetization leads to a similar behavior of the amplitude Δ_0^d. In addition, Cooper instability becomes typical for concentrations in the case where it is not manifested if the existence of the antiferromagnetic ordering in the system is not taken into account. On the other hand, the intensity of anomalous pairings decreases significantly in the presence of AFM.

The increase in the energy E_0 of localized states at the fixed concentration $n_e = 1.2$ and the same parameters J and V_0 as in Fig. 3 also leads to the destruction of the antiferromagnetic ordering (see Fig. 4a). In this case, this is because the occupation of localized states decreases as the localized level moves upward in the energy band. The superconducting ordering and the antiferromagnetic ordering compete at the chosen PAM parameters. This is reflected in Fig. 4a by the SOP maximum being attained at the point where the magnetization drops to zero.

Although the SC–AFM coexistence phase is realized, the SOP amplitude is significantly lower in the competition with the long-range antiferromagnetic order. The described dependence of the order parameters on the energy E_0 is related to experimental studies of HF systems. For example, the abovementioned compound $CeRhIn_5$ at atmospheric pressure is an antiferromagnet with the Néel temperature $T_N = 3.8\,K$ [41]. Under pressure, the Néel temperature of the sample first decreases weakly and then the long-range antiferromagnetic order is destroyed completely under the critical pressure $P_c = 1.75\,GPa$ [15]. This probably occurs through a first-order phase transition, which is a quantum phase transition at zero temperature. The SC–AFM coexistence phase is realized in a range of pressures that are less than the critical pressure P_c [16]. The pure superconducting phase was experimentally discovered under pressures that are greater than critical.

The picture shown in Fig. 4a qualitatively corresponds to the described studies. In this case, the energy

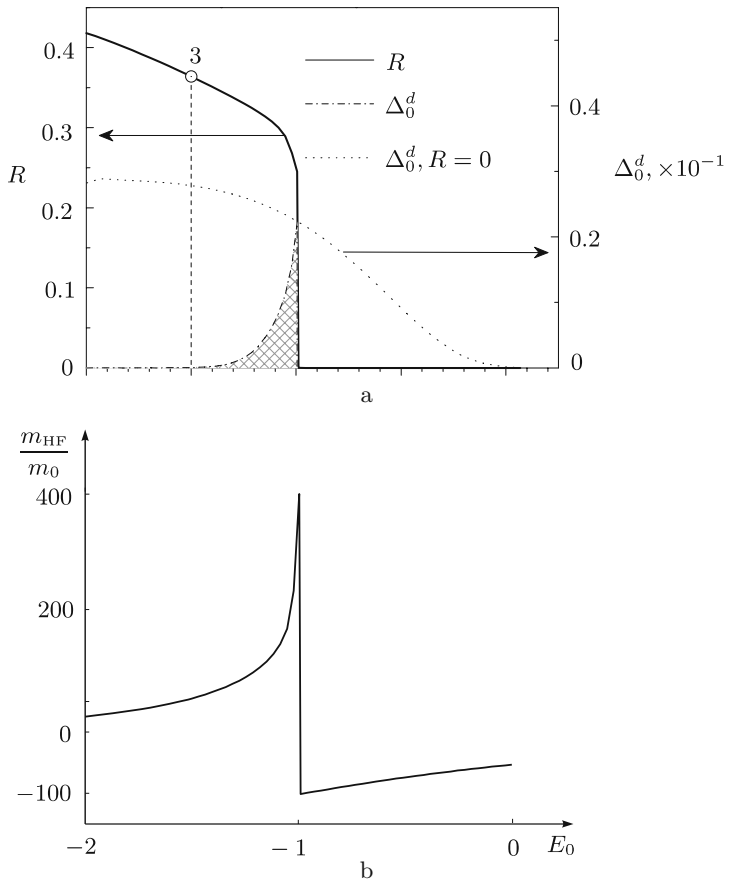

Fig. 4. (a) Dependence of the sublattice magnetization R and the SOP amplitude Δ_0^d on the energy E_0 of localized states. (b) The dependence of the effective mass of heavy quasiparticles normalized to the mass of the Bloch electron on the energy E_0.

E_0 of localized electrons plays the role of the main parameter, which varies under the external hydrostatic pressure. The mechanism for increasing the energy E_0 with increasing pressure is rather simple. It is well known that cerium is contained in the compound $CeRhIn_5$ as the Ce^{3+} ion. Therefore, the region around the ion has a large total positive charge. In view of the electrical neutrality condition, the nearest environment has an effectively negative charge. Under pressure, the Ce ion approaches the nearest environment, which causes an increase in the energy of the 4f electron located at this ion because of the Coulomb interaction. We also note that the increase in pressure can generally lead to changes in the amplitude t_{ml} of electron hopping between sites and in the hybridization parameter V_{ml} [22]. In our consideration, we assumed that the changes in these parameters with pressure make a smaller contribution to the formation of a certain type of ground state.

The effective mass of localized quasiparticles is an important characteristic of HF systems. The ratio of the effective mass of localized quasiparticles in the PAM to the mass of itinerant electrons in the parabolic-band approximation can be estimated using formula (16). The dependence of this quantity on the energy of the localized level is shown in Fig. 4b. Mass (16) becomes negative as the antiferromagnetic order is destroyed. In such a case, it was assumed that a transition to hole-type heavy quasiparticles occurs [40]. At each graph point, the values of the order parameter were recalculated in accordance with the diagram of the ground state shown in Fig. 4. It can be seen that as the antiferromagnetic order is destroyed, the effective mass increases with increasing E_0. In this case, the effective mass exhibits behavior resembling the

divergence at a critical point ($E_0 \approx -1$), above which the sublattice magnetization is zero. The effective mass decreases sharply in the passage through the critical point to the paramagnetic region, and its absolute value decreases afterwards.

An increase in the electron mass under external pressure was demonstrated based on a series of experiments made with the compound $CeRhIn_5$ [42], [43]. It was fixed at atmospheric pressure that the cyclotron mass of electrons exceeds the mass of the free electron by a factor of 5.5 [42]. This ratio could reach the value $m_c/m_0 = 100$ at the critical pressure. We note that the effective and cyclotron masses are equivalent in the parabolic-band approximation. The values of the effective mass in Fig. 4b, even if they exceed the values of the cyclotron mass, properly reflect the experimental pressure dependence of the mass qualitatively. We note that the increase in the effective mass of fermions in the described systems is related to the transition from the antiferromagnetic to the paramagnetic phase and to the decrease in the HF bandwidth.

7. Conclusions

Our study shows that the presence of the exchange coupling in the subsystem of localized fermions and the hybridization interaction between the localized and itinerant electrons suffices to realize the antiferromagnetic phase, the superconducting phase, and the SC–AFM coexistence phase. The position of the initial energy level of localized electrons with respect to the conduction-band bottom plays the role of the control parameter determining the phase transition to the ordered state for a given total electron concentration. The assumption that this parameter varies with increasing external pressure underlies the interpretation of the experimentally observed modification of the ground state structure of the HF compound $CeRhIn_5$ as a result of the quantum phase transition.

The diagram of system states contains the value of the control parameter in a vicinity of which the SC–AFM coexistence phase is realized. The approach of the control parameter to the critical value from the low-temperature range is accompanied by a rapid destruction of the long-range antiferromagnetic ordering with a simultaneous increase in the SOP. The presence of the long-range antiferromagnetic ordering is manifested in both the strong suppression of the amplitude of the anomalous Cooper averages and the modification of the Fermi energy spectrum. As a result, the superconducting gap is determined not only by the amplitude of the anomalous averages but also by the magnetization of the antiferromagnetic sublattice. This means that the superconducting gap in the SC–AFM coexistence phase is renormalized in two ways: the first way is related to the long-range magnetic order, and the second is related to a rearrangement of the Fermi excitation spectrum.

Acknowledgments. This work was supported by the Presidium of the Russian Academy of Sciences (Program "Quantum mesoscopic and disordered structures"), the Russian Foundation for Basic Research (Grant Nos. 10-02-00251 and 11-02-98007-RFFI-Sibir'), and the Ministry of Education and Science of the Russian Federation (Contract No. 14.132.21.1410).

REFERENCES

1. P. W. Anderson, *Science*, **235**, 1196–1198 (1987).
2. N. M. Plakida, *High-Temperature Cuprate Superconductors*: *Experiment, Theory, and Applications* (Springer Ser. Solid-State Sci., Vol. 166), Springer, Heidelberg (2010).
3. N. E. Alekseevskii and D. I. Khomskii, *Sov. Phys. Usp.*, **28**, 1136–1143 (1985).
4. G. R. Stewart, *Rev. Modern Phys.*, **56**, 755–787 (1987).
5. D. M. Newns and H. Read, *Adv. Phys.*, **36**, 799–849 (1987).
6. V. V. Val'kov and S. G. Ovchinnikov, *Quasiparticles in Strongly Correlated Systems* [in Russian], Izd. SO RAN, Novosibirsk (2001).
7. K. Miyake, S. Schmitt-Rink, and C. M. Varma, *Phys. Rev. B*, **34**, 6554–6556 (1986).

8. R. O. Zaitsev, *Sov. Phys. Solid State*, **29**, 2554–2556 (1987).
9. Yu. A. Izyumov, *Sov. Phys. Usp.*, **34**, 935–957 (1991).
10. S. V. Vonsovskii and M. S. Svirskii, *Sov. JETP*, **46**, 1619–1631 (1964).
11. A. I. Buzdin and L. N. Bulaevskii, *Sov. Phys. Usp.*, **29**, 412–425 (1986).
12. S. M. Hayden, L. Taillefer, C. Vettier, and J. Flouquet, *Phys. Rev. B*, **46**, 8675–8678 (1992).
13. R. Caspary, P. Hellmann, M. Keller, G. Sparn, C. Wassiew, R. Köhler, C. Geibel, C. Schank, F. Steglich, and N. E. Phillips, *Phys. Rev. Lett.*, **71**, 2146–2149 (1993).
14. G. Zwicknagl, A. N. Yaresko, and P. Fulde, *Phys. Rev. B*, **65**, 081103 (2002).
15. T. Park and J. D. Thompson, *New J. Phys.*, **11**, 055062 (2009); arXiv:0908.2404v1 [cond-mat.str-el] (2009).
16. T. Mito, S. Kawasaki, Y. Kawasaki, G.-Q. Zheng, Y. Kitaoka, D. Aoki, Y. Haga, and Y. Ōnuki, *Phys. Rev. Lett.*, **90**, 077004 (2003); arXiv:cond-mat/0211576v1 (2002).
17. Yu. A. Izyumov, N. M. Plakida, and Yu. N. Skryabin, *Sov. Phys. Usp.*, **32**, 1060–1083 (1989).
18. H. Mukuda, Y. Yamaguchi, S. Shimizu, Y. Kitaoka, P. Shirage, and A. Iyo, *J. Phys. Soc. Japan*, **77**, 124706 (2008); arXiv:0810.0880v1 [cond-mat.supr-con] (2008).
19. S. Shimizu, S. Tabata, H. Mukuda, Y. Kitaoka, P. M. Shirage, H. Kito, and A. Iyo, *J. Phys. Soc. Japan*, **80**, 043706 (2011); arXiv:1102.5282v1 [cond-mat.supr-con] (2011).
20. A. N. Lavrov, L. P. Kozeeva, M. R. Trunin, and V. N. Zverev, *Phys. Rev. B*, **79**, 214523 (2009).
21. M. B. Maple and O. Fisher, eds., *Superconductivity in Ternary Compounds*, Springer, Berlin (1982).
22. P. D. Sacramento, *J. Phys.*, **15**, 6285–6300 (2003).
23. J. V. Alvarez, *Phys. Rev. Lett.*, **98**, 126406 (2007).
24. C. M. Varma, W. Webber, and L. J. Randall, *Phys. Rev. B*, **33**, 1015–1019 (1986).
25. H. Tsunetsugu, M. Sigrist, and K. Ueda, *Rev. Modern Phys.*, **69**, 809–863 (1997).
26. V. A. Moskalenko, *Theor. Math. Phys.*, **116**, 1094–1107 (1998).
27. V. A. Moskalenko, *Theor. Math. Phys.*, **110**, 243–255 (1997).
28. V. V. Val'kov and D. M. Dzebisashvili, *Theor. Math. Phys.*, **157**, 1565–1576 (2008).
29. V. V. Val'kov and A. O. Zlotnikov, *Bull. Russ. Acad. Sci. Ser. Phys.*, **75**, 639–641 (2011).
30. N. N. Bogoliubov, *Collection of Scientific Works*: *Statistical Mechanics* [in Russian], Vol. 6, *Equilibrium Statistical Mechanics*: *1945–1986*, Nauka, Moscow (2006).
31. D. N. Zubarev, *Sov. Phys. Usp.*, **3**, 320–345 (1960).
32. N. M. Plakida, *Theor. Math. Phys.*, **5**, 1047–1052 (1970).
33. N. M. Plakida, *Theor. Math. Phys.*, **154**, 108–122 (2008).
34. R. Zwanzig, *Phys. Rev.*, **124**, 983–992 (1961).
35. H. Mori, *Prog. Theoret. Phys.*, **33**, 423–455 (1965).
36. R. O. Zaitsev, *Sov. Phys. JETP*, **41**, 100–103 (1975).
37. R. O. Zaitsev, *Sov. Phys. JETP*, **43**, 574–579 (1976).
38. T. Park, E. D. Bauer, and J. D. Thompson, *Phys. Rev. Lett.*, **101**, 177002 (2008); arXiv:0806.3308v1 [cond-mat.supr-con] (2008).
39. V. V. Val'kov and D. M. Dzebisashvili, *Theor. Math. Phys.*, **162**, 106–125 (2010).
40. V. V. Val'kov and D. M. Dzebisashvili, *JETP*, **110**, 301–318 (2010).
41. H. Hegger, C. Petrovich, E. G. Moshopoulou, M. F. Hundley, J. L. Sarrao, Z. Fisk, and J. D. Thompson, *Phys. Rev. Lett.*, **84**, 4986–4989 (2000).
42. H. Shishido, R. Settai, H. Harima, and Y. Ōnuki, *J. Phys. Soc. Jap.*, **74**, 1103–1106 (2005).
43. G. Knebel, D. Aoki, J.-P. Brison, and J. Flouquet, *J. Phys. Soc. Jap.*, **77**, 114704 (2008); arXiv:0808.3687v1 [cond-mat.str-el] (2008).